

# CHAPTER 1

---

## Delaunay triangulations in the plane

---

### 1.1 The Voronoi Diagram

**Definition:** Consider a finite set  $S = \{p_1, \dots, p_n\} \subseteq \mathbb{R}^2$  of  $n$  distinct points in the plane. The *Voronoi cell*  $V_i$  of  $p_i \in S$  is the set of points  $x$  that are closer to  $p_i$  than to any other points of the set:

$$V_i = \{x \in \mathbb{R}^2 \mid \|x - p_i\| < \|x - p_j\|, \forall 1 \leq i \leq n, i \neq j\}$$

where  $\|x - y\|$  is the euclidian distance between  $x$  and  $y$ .

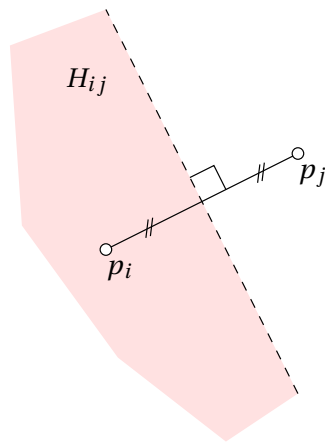


Figure 1.1: Points  $p_i$  and  $p_j$ , their perpendicular bisector (in dashed lines) and half-plane  $H_{ij}$ .

Consider first the case where  $S = \{p_i, p_j\}$ . The perpendicular bisector of the line segment  $p_i p_j$  is a line perpendicular to  $p_i p_j$  and passing through its midpoint. The

perpendicular bisector of  $p_i p_j$  divides  $\mathbb{R}^2$  into two halfplanes  $H_{ij}$  and  $H_{ji}$ :

$$H_{ij} = \{x \in \mathbb{R}^2 \mid \|x - p_i\| < \|x - p_j\|\}.$$

Here, we have clearly  $V_i = H_{ij}$ . The perpendicular bisector of line segment  $p_i p_j$  is the intersection of the closures of the two half planes:  $\overline{H_{ij}} \cap \overline{H_{ji}}$ .

Let's make the problem a little more complicated and consider a set  $S = \{p_i, p_j, p_k\}$  of 3 points. The Voronoi cell associated to  $p_i$  is the intersection of half planes  $H_{ij}$  and  $H_{ik}$ :  $V_i = H_{ij} \cap H_{ik}$  (see Figure 1.2).

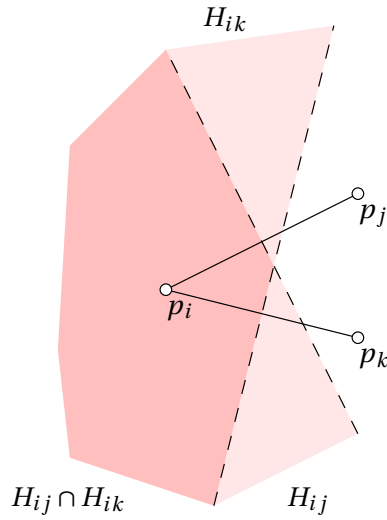


Figure 1.2: Points  $p_i, p_j$  and  $p_k$  and their perpendicular bisectors.

In the general case, the Voronoi cell relative to  $p_i$  is the intersection of all half planes:

$$V_i = \bigcap_{1 \leq j \leq n, j \neq i} H_{ij}. \quad (1.1)$$

By definition (1.1), each Voronoi cell  $V_i$  is the intersection of open half planes containing vertex  $p_i$ . The intersection of two convex polygon being itself a convex polygon,  $V_i$  is therefore *a convex polygon*.

**Definition:** *The Voronoi diagram  $V(S)$  is the unique subdivision of the plane into  $n$  cells is the union of all Voronoi cells  $V_p$ :*

$$V = \bigcup_{1 \leq i \leq n} V_i. \quad (1.2)$$

Each point  $x \in \mathbb{R}^2$  having at least one closest point in  $S$ , the Voronoi diagram covers the entire plane. Different Voronoi regions are disjoint. Therefore, the Voronoi diagram is unique.

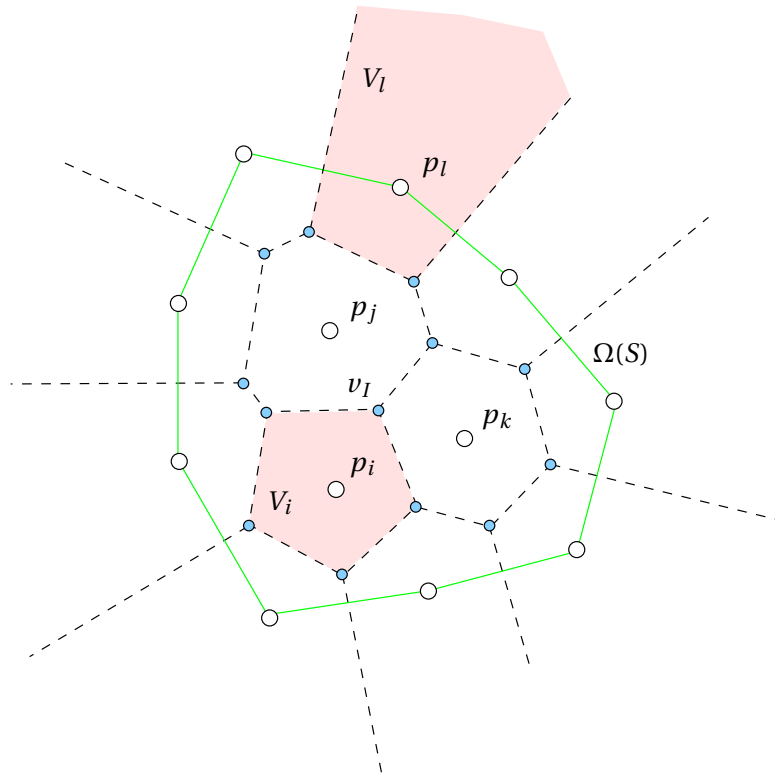


Figure 1.3: Voronoi Diagram. Voronoi cell  $V_i$  is closed because it correspond to point  $p_i$  that is not on  $\Omega(S)$ . Voronoi cell  $V_l$  is open because  $p_l \in \Omega(S)$ .

**Definition:** The *convex hull*  $\Omega(S)$  of a finite point set  $S$  is the smallest convex polygon that contains  $S$ .

Voronoi cells are either closed or open. They can only be open for points (like  $p_l$  in see Figure 1.3) that are located on the convex hull  $\Omega(S)$  of the point set.

## 1.2 Triangulations

**Definition:** A triangulation  $T(S)$  of  $S$  is a set of non overlapping triangles that exactly covers the convex hull  $\Omega(S)$  with all points of  $S$  being among the vertices of the triangulation.

Different triangulations of the same point set  $S$  may exist (e.g. Figure 1.4), but we are going to show that they all have the same number of edges and of triangles.

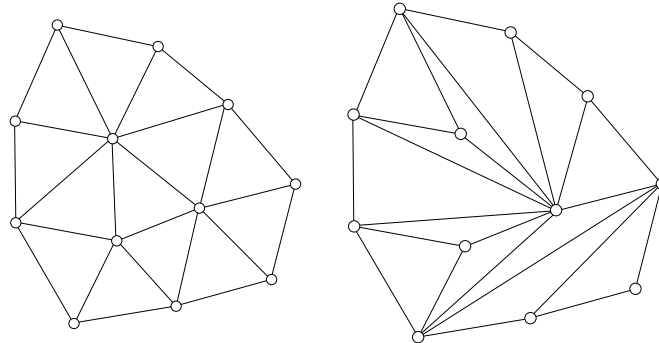


Figure 1.4: Two triangulations of the same point set, both containing  $n_f = 13$  triangles defined by a total of  $n = 12$  points with  $n_h = 9$  points that lie on  $\Omega(S)$ .

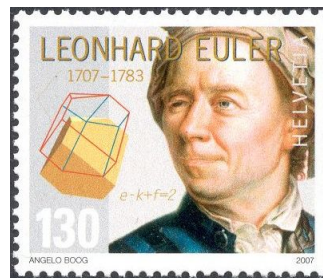


Figure 1.5: Commemorative stamp with Euler and its formula.

**Property 1.2.1** Every triangulation  $T(S)$  contains exactly  $n_f = 2(n-1) - n_h$  triangles and  $n_e = 3(n-1) - n_h$  edges.

**Proof** The proof uses a very well know result of Euler that he proved in 1758. Here is what Euler had to say: Consider any polyhedron and let  $n$  be the number of its vertices,  $n_f$  the number of its faces, and  $n_e$  be the number of its edges. Then

$$n + n_f - n_e = 2. \quad (1.3)$$

A commemorative stamp put out by the Swiss Post shows Euler together with that very famous formula (Figure 1.5). David Eppstein gives 20 different proofs of Euler's formula in [?]. Here is one that is quick and elegant. The skeleton of any convex polyhedron is a planar graph. This is geometrically easy to see: in order tu build such a planar graph, dispose the polyhedron on one on a plane and dig a hole on one of its face (an upper face). Then, enlarge this hole in order to unfold the polyhedron up to the point it is completely flattened. The upper face then becomes "infinite" and can be seen as the outer face of the graph. Figure 1.6 shows an example of such a flattening procedure: a cube is shown with its corresponding skelton that is actually

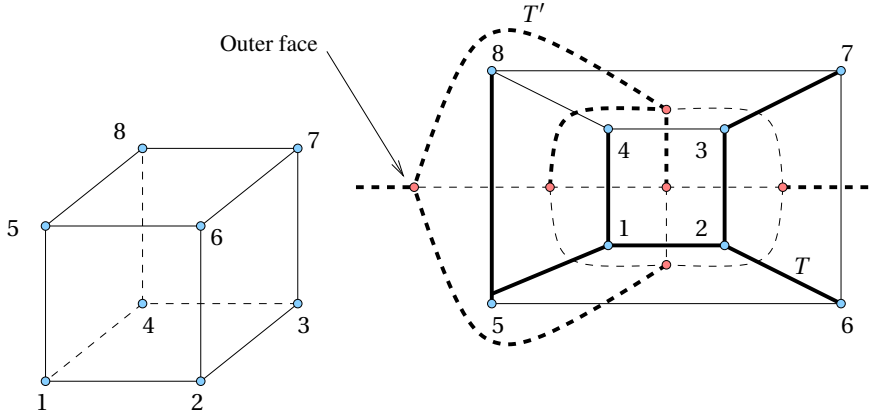


Figure 1.6: A cube (left) and its corresponding skelton  $\Gamma$  (right, plain lines) and the dual  $\Gamma'$  of  $\Gamma$  (right, dashed lines). Edges in bold correspond to a spanning tree  $T$  of  $\Gamma$  and edges in bold and dashed correspond to a spanning tree of  $\Gamma'$ .

a planar graph  $\Gamma$ . Let  $\Gamma'$  be the dual of  $\Gamma$  i.e. a graph with its 6 nodes that correspond to the faces of the cubes and its 12 edges that correspond to the edges of the cube. Edges of both graphs have a one-to-one correspondance.

Let  $T$  be a spanning tree of  $\Gamma$  i.e. a subgraph  $T \subset \Gamma$  that includes all of the vertices of  $\Gamma$  and that is a tree i.e. that contains no cycles.  $T$  does not contain any cycles, so it does not disconnect the plane. The co-tree  $T^*$  of  $T$  is the set of edges of the graph that are not in  $T$ . Consider now the set of edges  $T' \subset \Gamma'$  that correspond to  $T^*$ . Set  $T'$  contains no cycles: if one cycle exists in  $T'$ , then the corresponding edges of  $\Gamma$  would create some isolated vertices in  $T$ , which is impossible because  $T$  is a spanning tree and it contains all vertices of  $\Gamma$ .  $T'$  contains all vertices (the faces of the polyhedron) of  $\Gamma'$  because  $T$  does not contain any cycles. Then,  $T'$  is a spanning tree of  $\Gamma'$ .

The number of edges on a spanning tree can be computed in a general fashion. Let's construct a spanning tree in the following way: start with one random edge  $e$  of  $\Gamma$  and add it to  $T$ . This first edge  $e$  connects 2 vertices that are inserted in a stack. While this stack is not empty, we take the vertex  $v$  at the top of the stack and look for all edges  $e_i(v, v_i)$  that are incident to  $v$ . We add  $e_i$  to  $T$  if neither  $v$  or  $v_i$  is not yet in  $T$ . So, each edge of  $T$  correspond to one vertex of  $\Gamma$ , except the first one that correspond to two. Then, a spanning tree has exactly  $n - 1$  vertices.

So  $T$  has  $n$  vertices and  $k \equiv n - 1$  edges. Similarly,  $T'$  has  $n_f$  vertices and  $k' \equiv n_f - 1$  edges. Since  $k + k' = n_e$ , we have  $n - 1 + n_f - 1 = n_e$  and formula 1.3 follows.

Euler's formula applies to polyhedron i.e. meshes that are topologically equivalent to a sphere. Euler generalized its formula to general orientable manifolds as

$$n - n_e + n_f = \chi. \tag{1.4}$$

Here,  $\chi$  is the Euler characteristic is a topological invariant: it is a number that de-

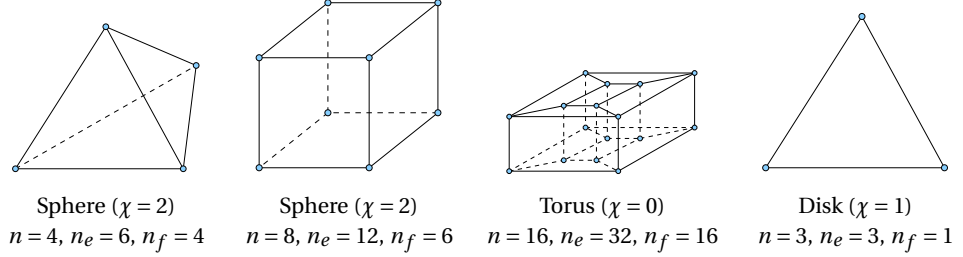


Figure 1.7: Computation of Euler's characteristic  $\chi$  for different manifold meshes.

describes the topological structure of the domain. For a sphere, we have obviously  $\chi = 2$ . In this section, we are essentially concerned by domains that are topologically equivalent to a disk i.e. when  $\chi = 1$ . Figure 1.7 shows manifold meshes of different objects together with their Euler characteristic.

Now let's specialize Euler's formula to triangulations. In the case of a triangulation of a closed manifold (a sphere or a torus), every edge is connected to 2 triangles and each triangle has 3 incident edges. We have then

$$2n_e = 3n_f.$$

This last result combined with Euler's formula gives, for a closed manifold

$$n_f = 2(n - \chi) \text{ and } n_e = 3(n - \chi).$$

For planar triangulations, we consider domains that are topologically equivalent to the a disk i.e. where  $\chi = 1$ . Those domains have one boundary and every edge of the boundary of the domain of is connected to one single triangle. Assume that  $n_h$  is the number of edges (or of points) of the boundary. In this case,  $n_e - n_h$  edges are internal with two adjacent triangles and  $n_h$  edges and have only one adjacent triangle. Every triangle being always incident to 3 edges, we get the following result

$$3n_f = 2(n_e - n_h) + n_h. \quad (1.5)$$

Combining Euler's formula (1.4) with (1.5) gives the result  $n_f = 2(n - 1) - n_h$  and  $n_e = 3(n - 1) - n_h$ . ■

### 1.3 The Delaunay triangulation

The Delaunay triangulation  $DT(S)$  is the geometric dual of the Voronoi diagram (see Figure 1.8). The Voronoi diagram  $V$  is made of  $n$  Voronoi cells  $V_i$  that correspond to the points  $p_i$ ,  $1 \leq i \leq n$  of  $S$ . The line segments that form the boundaries of Voronoi cells and are the Voronoi edges. Voronoi edges are orthogonal bisectors of neighboring points in the diagram. The endpoints of the Voronoi edges are called Voronoi vertices  $v_I$ ,  $1 \leq I \leq N$ ,  $N$  being the number of Voronoi vertices. Voronoi vertices  $v_I$  are those points that are equidistant to three or more vertices.

**Definition:** Points of  $S$  are said to be *in general position* if there exist no quadruplet of points of  $S$  that are co-circular.

When the points of  $S$  are in general position, Voronoi vertices are *triple points* i.e. they are equidistant of three points of  $S$ . Consider a Voronoi Vertex  $v_I$  that is equidistant to points  $p_i, p_j$  and  $p_k \in S$  (see Figure 1.3). Voronoi point  $v_I = H_{ij} \cap H_{jk} \cap H_{ki}$  is the circumcenter of a triangle  $\Delta_I = p_i p_j p_k$ .

**Definition:** The Delaunay triangulation  $DT(S)$  is the triangulation of  $S$  that consist in the union of the  $N$  triangles  $\Delta_I, 1 \leq I \leq N$  that correspond to the triple points of the Voronoi diagram (see Figure 1.8).

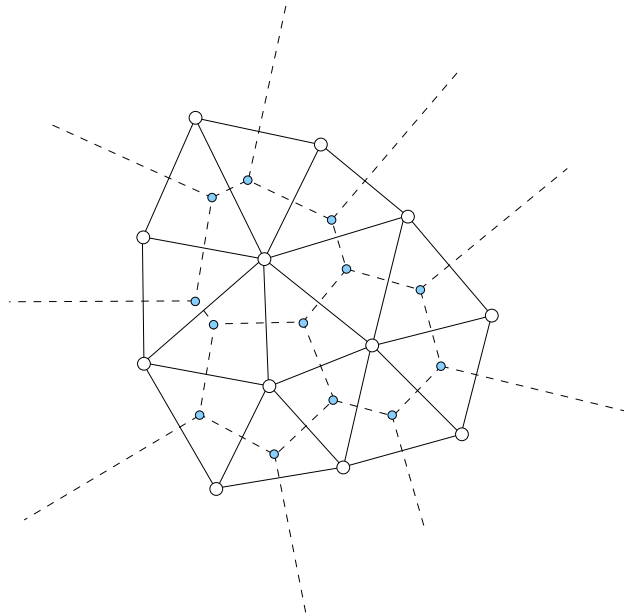


Figure 1.8: Voronoi Diagram (in dashed lines) and Delaunay triangulation. White points are points of  $S$  and blue points are Voronoi vertices that are the circumcenters of the triangles.

We should now show that the set of triangles in question is a triangulation in the sense of Definition 1.2. If this is the case, then Property 1.2.1 applies and  $N = 2(n - 1) - n_h$ . The fact that  $DT$  is a triangulation will be the consequence of the following properties of the Delaunay triangles. The fact that  $DT$  is a triangulation will be the consequence of the two following properties.

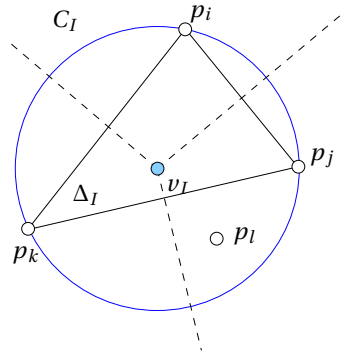


Figure 1.9: Illustration of why the empty circle property is true.

### 1.3.1 The empty circumcircle property

We will first demonstrate the following remarkable result that is called the empty circumcircle property.

**Property 1.3.1** *The empty circumcircle of any triangle in the Delaunay triangulation is empty i.e. it contains no point of  $S$ .*

**Proof** Consider the Delaunay triangle  $\Delta_I = p_i p_j p_k$  (see Figure 1.9). Assume now that point  $p_l \in C_I$  where  $C_I$  is the circumcircle of  $\Delta_I$ . By definition, the triple point  $v_I$  is at equal distance to  $p_i$ ,  $p_j$  and  $p_k$  and no other points of  $S$  are closer to  $v_I$  than those three points. Then, if a point like  $p_l$  exist in  $S$ ,  $v_I$  is not a triple point and triangle  $\Delta_I$  cannot be a Delaunay triangle.

### 1.3.2 Delaunay Edges

It is useful at that point to look at some geometrical properties of circle bundles that share two points  $p_i$  and  $p_j$ . The centers of such circles lie on the perpendicular bisectors of line segment  $p_i p_j$  (see Figure 1.10). Edge  $p_i p_j$  divides disk  $C_1$  into two disk sectors and one of the two sectors completely lies inside  $C_2$ . On the Figure, the pink sector of  $C_1$  is inside  $C_2$  and the yellow sector of  $C_2$  lies inside  $C_1$ .

**Definition:** An edge  $p_i p_j$  of a triangulation is a *Delaunay edge* if there exist a circle that contains  $p_i$  and  $p_j$  and that is empty i.e. that contain no point of  $S$ .

**Property 1.3.2** *A mesh is a Delaunay Triangulation if and only if all its edges are Delaunay edges.*

**Proof** Let us first show that a Delaunay triangulation has only Delaunay edges. Assume a Delaunay triangulation  $T(S)$  and an edge  $p_i p_j$  that is not Delaunay. This means that there exist no circle passing through  $p_i$  and  $p_j$  that is empty. Consider



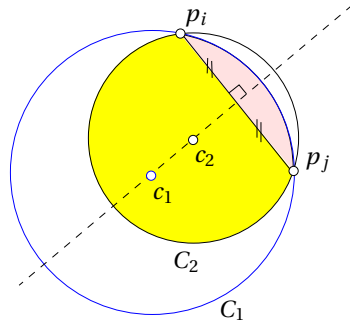


Figure 1.10: Two circles  $C_1$  and  $C_2$  sharing an edge  $p_i p_j$ . The centers of the circles  $c_1$  and  $c_2$  lie on the perpendicular bisector of segment  $p_i p_j$  (in dashed lines).

Delaunay triangle  $\Delta_I = p_i p_j p_k$  that contains edge  $p_i p_j$ . Its circumcircle is empty by definition because  $T$  is a Delaunay triangulation. This is in contradiction with the hypothesis that there exist no circle passing through  $p_i$  and  $p_j$  and that is not empty.

Now let's prove that if every edge of a triangulation is Delaunay, then every triangle is Delaunay as well. Assume that triangle  $\Delta_I = p_i p_j p_k$  is not Delaunay, but all its 3 edges  $p_i p_j$ ,  $p_i p_k$  and  $p_j p_k$  are Delaunay. Figure 1.11 shows a configuration with a non Delaunay triangle  $\Delta_I = p_i p_j p_k$  which circumcircle contains  $p_l$ . Because we deal with triangulations as defined in Definition 1.2,  $p_l$  cannot be inside triangle  $\Delta_I$ . It is then situated inside one of the three circular sectors delimited by  $p_i$ ,  $p_j$  and  $p_k$ . Assume that  $p_l$  and  $p_j$  are on opposite sides of  $p_i p_k$  like in Figure 1.11. By hypothesis, there exist a circle passing through  $p_i$  and  $p_k$  and that is empty. The center of such a circle lies on the orthogonal bisector of  $p_i p_k$ . Any circle like  $C_1$  with its center  $c_1$  that is below  $c_I$  contains  $p_j$  any circle  $C_2$  that is above  $c_I$  contains  $p_l$ , which is in contradiction with the hypothesis that there exist a circle passing through  $p_i p_k$  and that is empty.

### 1.3.3 Local Delaunayhood

**Definition:** Given a triangulation  $T(S)$  and an edge  $p_i p_j$  in the triangulation that is adjacent to two triangles  $\Delta_I = p_i p_j p_k$  and  $\Delta_J = p_i p_l p_j$ . We call edge  $p_i p_j$  *locally Delaunay* if  $p_l$  lies on or outside the circumcircle of  $\Delta_I$ .

Figure 1.12 gives an illustration of an edge  $p_i p_j$  that is not locally Delaunay: point  $p_l$  lies inside circle  $C_I$ . It is easy to see that this condition is symmetric: if point  $p_l$  lies inside circle  $C_I$ , then point  $p_k$  lies inside circle  $C_J$ . We'll prove that below.

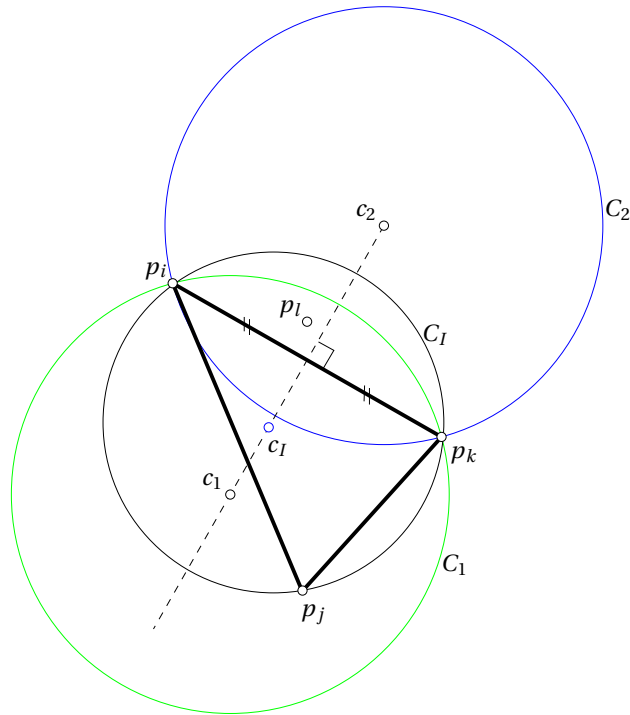


Figure 1.11: Two circles  $C_1$  and  $C_2$  sharing an edge  $p_i p_j$ . The centers of the circles  $c_1$  and  $c_2$  lie on the perpendicular bisector of segment  $p_i p_j$ .

### 1.3.4 Edge Flip

Consider again the situation of two triangles adjacent to edge  $p_i p_j$  as depicted in Figure 1.12. Flipping edge  $p_i p_j$  consist in replacing triangles  $p_i p_j p_k$  and  $p_j p_i p_l$  by triangles  $p_l p_k p_i$  and  $p_k p_l p_j$ . Edge  $p_i p_j$  has been flipped and replaced by edge  $p_k p_l$ .

The edge flip operator can only be applied to a pair of triangles that form a convex quadrilateral. If it is concave, then flipping the edge leads to an invalid configuration with two overlapping triangles (see Figure 1.13).

**Property 1.3.3** *An edge that is not locally Delaunay is flippable and the new edge resulting of the flip operation is locally Delaunay.*

**Proof** Let us first show that any edge that is not locally Delaunay is flippable. Consider Figure 1.12. Edge  $p_i p_j$  is not locally Delaunay because  $p_k \in C_j$  and  $p_l \in C_i$ . A simple way of checking whether edges  $p_i p_j$  and  $p_k p_l$  can be flipped is to verify that they actually intersect. Consider triangle  $p_j p_k p_i$  on Figure 1.12. The fact that  $p_l$  is on the opposite side of  $p_i p_j$  than  $p_k$  and that it lies inside  $C_1$  ensures that  $p_k p_l$  in-

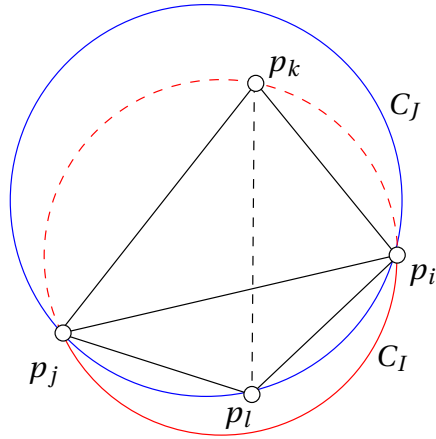


Figure 1.12: An edge  $p_i p_j$  that is not locally Delaunay.

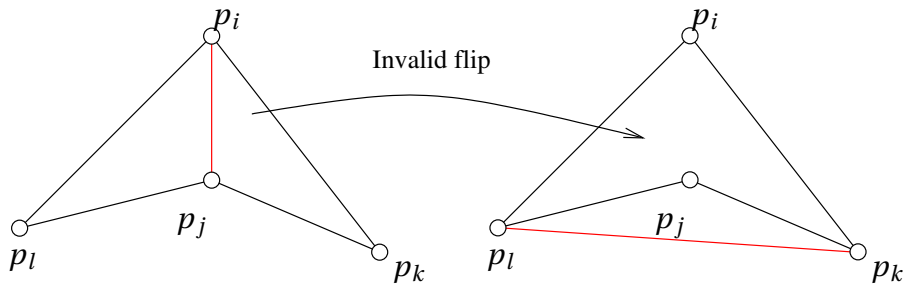


Figure 1.13: Invalid edge flip configurations.

intersects  $p_i p_j$  which proves that edge  $p_i p_j$  is flippable if  $p_i p_j$  is not locally Delaunay. Move now to Figure 1.14. and prove that, if  $p_i p_j$  is not locally Delaunay, then  $p_k p_l$  is locally Delaunay. In other words, we'd like to prove that, provided that  $p_l$  is inside  $C$ , then  $p_i$  is outside  $C'$ .

Circles  $C$  and  $C'$  share edge  $p_k p_j$  and points  $p_i$  and  $p_l$  are on the same sides of edge  $p_k p_j$ . Edge  $p_i p_j$  is not Delaunay by hypothesis. Then point  $p_l$  is inside  $C$ , as well as the whole arc  $\widehat{p_k p_l p_j}$  (in dashed line on Figure 1.14) of  $C'$ . Point  $p_i$  belongs to  $C$  and is on the same side of  $p_k p_j$  as  $p_l$ , it is then outside  $C'$  and edge  $p_k p_l$  is locally delauday. ■

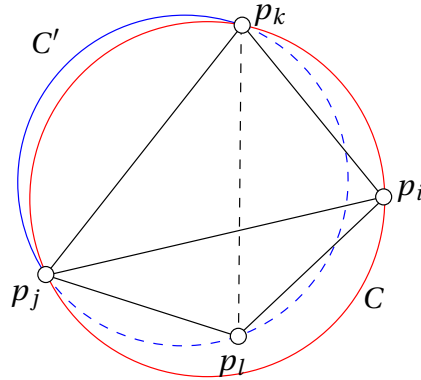


Figure 1.14: If  $p_i p_j$  is not locally Delaunay, then  $p_k p_l$  is locally Delaunay.

### 1.3.5 Locally Delaunay vs. Globally Delaunay

**Property 1.3.4** *If all edges of triangulation  $T(S)$  are locally Delaunay, then  $T$  is the Delaunay triangulation  $DT(S)$ .*

The fact that a specific edge is locally Delaunay does not imply that both its two adjacent triangles are Delaunay triangles. Yet, if all edges are locally Delaunay, then the resulting triangulation is Delaunay.

**Proof** We prove property 1.3.4 by contradiction. Assume all edges of a triangulation to be locally Delaunay. Assume that triangle  $\Delta_I = p_i p_j p_k$  has its circumcircle  $C_I$  that contains point  $p_l \in S$ . The situation is summarized on Figure 1.15. Assume that point  $p_l$  and  $p_i$  are on opposite sides of  $p_j p_k$ . Edge  $p_j p_k$  is locally Delaunay but triangle  $p_i p_j p_k$  is not Delaunay because its circumcircle is not empty (it actually contains point  $p_l$ ). Consider triangle  $p_k p_j p_m$ . Points  $p_i$  and  $p_m$  are on opposite sides of  $p_j p_k$  and  $p_m$  is outside  $C_I$ . This implies that  $C_I$  contains  $p_l$  as well. We can continue that and show that  $C_K$  and  $C_L$  both contain  $p_l$  as well. Yet, edge  $p_0 p_n$  is supposed to be locally Delaunay which means that  $p_l$  should be outside  $C_L$ . This is indeed a contradiction.

### 1.3.6 The Flip Algorithm

Result 1.3.4 is of high importance. Combined with the flip algorithm, we can foresee a simple algorithm that would start with any triangulation  $T(S)$  and would produce the Delaunay triangulation  $DT(S)$  using edge successive flips. The algorithm could be summarized as follows

- Insert all the internal edges of  $T(S)$  in a stack.
- Do while the stack is not empty

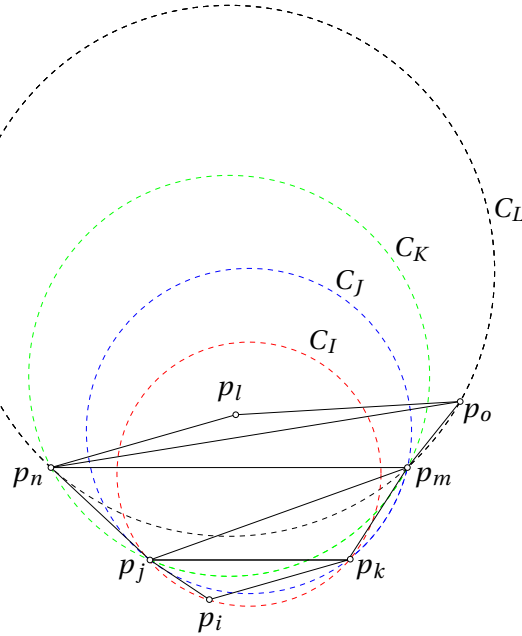


Figure 1.15: An edge  $p_i p_j$  that is locally Delaunay (point  $p_m$  is outside  $C_I$ ) but with triangle  $p_i p_j p_k$  that is not Delaunay.

- Take edge  $p_i p_j$  at the top of the stack. This edge is adjacent to triangles  $p_i p_j p_k$  and  $p_j p_i p_l$ . If  $p_i p_j$  is not locally Delaunay, then flip it and add edges  $p_i p_k, p_k p_j, p_j p_l$  and  $p_l p_i$  in the stack. If one of those edges was already present in the stack, update its neighbors.
- Remove  $p_i p_j$  from the stack.

Two questions should be asked at that point: (i) does this algorithm produce the Delaunay triangulation of  $S$  and (ii) if it achieves to create  $DT(S)$ , what is its complexity?

**Proposition 1.3.1** *The edge flip algorithm converges to  $DT(S)$  in at most  $\mathcal{O}(n^2)$  flips.*

**Proof** Consider an edge  $p_i p_j$  that is not Delaunay (Figure 1.16) with its two adjacent triangles  $p_i p_j p_k$  and  $p_j p_i p_l$  and their respective circumcircles  $C_I$  and  $C_J$ , with  $p_l \in C'_j$  and  $p_k \in C'_i$ . Edge flip will produce triangles  $p_j p_k p_l$  and  $p_i p_l p_k$  and their respective circumcircles  $C'_I$  and  $C'_J$ . Edge  $p_k p_l$  is locally Delaunay i.e.  $p_i \notin C'_I$  and  $p_j \notin C'_J$ .

Consider now the set of all possible point-triangle relations in a mesh  $T$  and a function  $F(T)$  that counts how many of those relations violate the Delaunay empty circle property. There is at most  $\mathcal{O}(n^2)$  point-triangle pairs in a mesh (see property 1.2.1). So,  $F$ 's magnitude is not bigger than  $\mathcal{O}(n^2)$ . Assume now that edge  $p_i p_j$  is

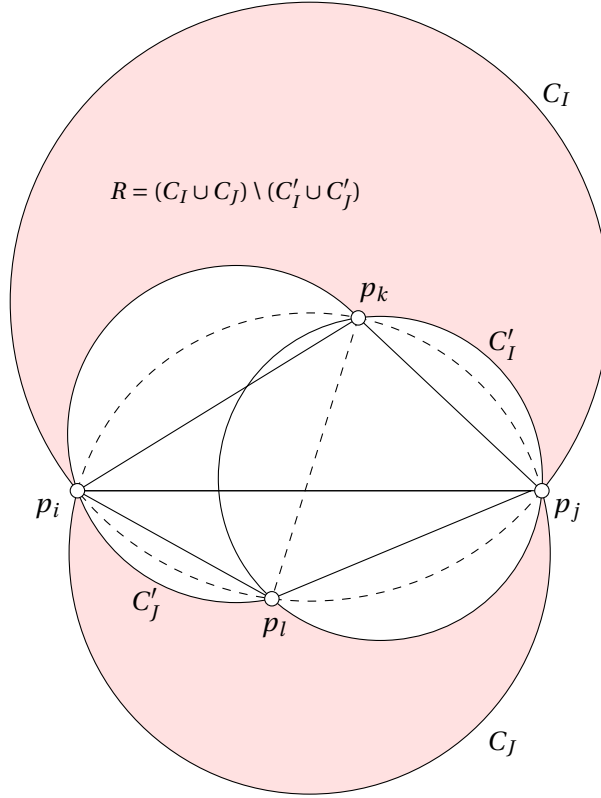


Figure 1.16: Edge flip:  $C_I \cup C_J \subset C'_I \cup C'_J$ .

flipped, leading to a new triangulation  $T'$ . Flipping an edge always leads to  $F(T') < F(T)$ . Figure 1.16 shows visually that

$$C_I \cup C_J \subset C'_I \cup C'_J,$$

the colored zone in the Figure representing

$$R = (C_I \cup C_J) \setminus (C'_I \cup C'_J).$$

If some points of  $S$  were inside circumcenters of triangles  $p_i p_j p_k$  and  $p_j p_i p_l$  in  $T$ , then edge flip will not increase that number because those points will not be anymore invalid. If  $R$  contains no points of  $S$ , then  $F(T') = F(T) - 2$  because the two point-triangle relations associated to points  $p_l$  and  $p_k$  and triangles  $p_i p_j p_k$  and  $p_j p_i p_l$  disappear from  $F$ . In conclusion, we have

$$F(T') \leq F(T) + 2$$

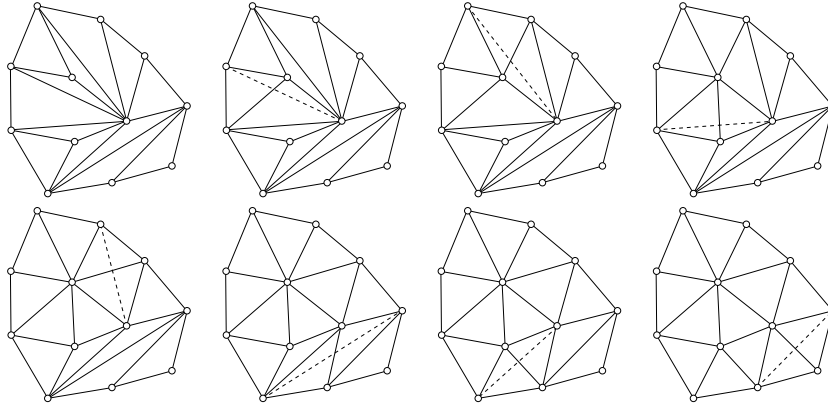


Figure 1.17: Building an angle-optimal triangulation using swaps.

which means that  $F$  decreases at each edge flip.

$F$  is bounded by above by  $\mathcal{O}(n^2)$ . It is also bounded by below: only the Delaunay triangulation has empty circumcircles,  $F(\text{DT}) = 0$ . The edge flip algorithm converges to the Delaunay triangulation and its complexity is  $\mathcal{O}(n^2)$  in the worst case. ■

This result is of utmost importance. It means that every triangulation  $T(S)$  is connected to the Delaunay triangulation  $\text{DT}(S)$  by at most  $\mathcal{O}(n^2)$  flips. It also means that any two triangulations  $T$  and  $T'$  are flip connected. Both  $T$  and  $T'$  being connected to  $\text{DT}$ , it is therefore possible to go from  $T$  to  $\text{DT}$  using flips and then from  $\text{DT}$  to  $T'$  using “back flipping”. The flip-connectness of 2D triangulations allows to generate meshes of arbitrary domains with low complexity. This will be developed in further chapters. Figure 1.17 illustrates the edge flip procedure.

### 1.3.7 The MaxMin property

Let us first recall a very old geometry theorem from Thales.

**Proposition 1.3.2** *Let  $C_A$  and  $C_B$  be two circumcircles of edge  $p_i p_j$  (see Figure 1.18). Let  $b_1$  and  $b_2$  be two points on  $C_B$  on the same side of  $p_i p_j$ . Then,  $b_1$  and  $b_2$  see the edge  $p_i p_j$  with the same angle  $\beta$ . Consider now point  $a$  on the same side of  $p_i p_j$  as  $b_1$  and  $b_2$  but on circle  $C_A$ . Assume that  $b_1, b_2$  are inside  $C_A$ . Then,  $\alpha < \beta$ .*

Consider a triangulation  $T(S)$  with  $n_f$  triangles. This triangulation has  $3n_f$  internal angles (3 angles per triangle). Consider the vector of angles  $A(T) = (\alpha_1, \dots, \alpha_{3n_f})$  sorted by increasing values. We can define such a vector for any triangulation. Each triangulation  $T(S)$  has the same number of triangles so each vector  $A(T)$  has the same length and it is therefore possible to compare them, e.g. lexicographically. We say that one given triangulation  $T$  is angle-optimal if  $A(T) \leq A(T'), \forall T'$ .

**Property 1.3.5** *The Delaunay triangulation  $\text{DT}(S)$  is angle-optimal: it maximizes the minimum angle among all possible triangulations.*

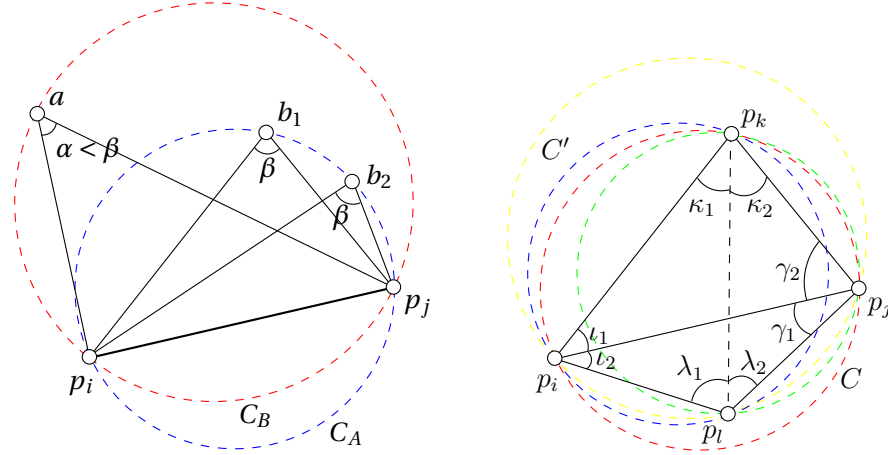


Figure 1.18: Thales theorem (left) and MaxMin property illustrated (right)

**Proof** Consider two triangulations  $T$  and  $T'$ , where  $T'$  differs from  $T$  by one edge flip. Let us prove that  $A(T') \leq A(T)$ . The edge flip procedure consist in replacing triangles  $p_i p_j p_k$  and  $p_j p_l p_k$  by triangles  $p_k p_l p_i$  (see Figure 1.18). The angles of the old configuration are respectively

$$\kappa_1 + \kappa_2, \gamma_2, \iota_1, \iota_2, \gamma_1 \text{ and } \lambda_1 + \lambda_2.$$

The angles of the old configuration are respectively

$$\iota_1 + \iota_2, \kappa_1, \lambda_1, \kappa_2, \lambda_2 \text{ and } \gamma_1 + \gamma_2.$$

Our aim is to bound by above all angles of the old configuration. Two of the 6 relations are obvious:  $\gamma_1, \gamma_2 < \gamma_1 + \gamma_2$  and  $\iota_1, \iota_2 < \iota_1 + \iota_2$ . We use Thales Theorem 1.3.2 for the last four ones. Thales Theorem applied respectively to segments  $p_i p_l$  (blue and yellow circles),  $p_j p_k$  (red and green circles),  $p_i p_k$  (blue and red circles) and  $p_l p_j$  (yellow and green circles) gives

$$\gamma_1 < \kappa_1, \iota_1 < \lambda_2, \gamma_2 < \lambda_1 \text{ and } \gamma_1 < \kappa_1$$

which are the four relations that were needed. Successive edge flips lead to the Delaunay triangulation and each flip does not increase the minimum angle. The Delaunay triangulation is therefore angle-optimal. ■